Available online at www.sciencedirect.com
SCIENCE DIRECT®
Physics Letters A 346 (2005) 321–326
PHYSICS LETTERS A
www.elsevier.com/locate/pla

Internal friction evidence of uncorrelated magnetic clusters in electron-doped manganite $Sr_{0.8}Ce_{0.2}MnO_3$

W.J. Lu *, B.C. Zhao, R. Ang, W.H. Song, J.J. Du, Y.P. Sun

Key Laboratory of Materials Physics, Institute of Solid State Physics, Chinese Academy of Sciences, Hefei 230031, PR China

Received 8 June 2005; accepted 29 July 2005

Available online 15 August 2005

Communicated by J. Flouquet

Abstract

Electron-doped manganite $Sr_{0.8}Ce_{0.2}MnO_3$ has been systematically investigated by X-ray diffraction, electronic transport, magnetic, internal friction, and Young's modulus experiments. The X-ray diffraction result indicates that the compound remains tetragonal (I4/mcm) structure at room temperature. Due to the strong Jahn–Teller (JT) distortion, the ground state is antiferromagnetic (AFM) insulator. Below 20 K, a spin-glass (SG) state dominates at low temperatures. In the paramagnetic (PM) region, an internal friction peak at around 250 K, which is characteristic of relaxation, has been observed. Under applied magnetic field, the internal friction peak moves to higher temperature, which is suggested to originate from the formation of ferromagnetic (FM) clusters in PM region. In addition, the softening of Young's modulus in the vicinity of AFM transition temperature is interpreted in terms of the strong electron–phonon interaction.

PACS: 75.47.Lx; 75.30.Kz; 62.40.+i

Keywords: Manganites; Magnetic clusters; Phase separation; Internal friction

1. Introduction

Hole-doped manganese oxides $R_{1-x}A_xMnO_3$ (R = rare-earth ions; A = divalent ions such as Ca, Sr, Ba, Pb, etc.) with a perovskite structure have stimulated considerable scientific and technological interest because of their exotic electronic and magnetic properties [1–4]. These manganites present a colossal magnetoresistance (CMR) effect and the characteristic feature of the CMR manganites is the strong interaction between charge carriers in the e_g band, localized spins of t_{2g} electrons, and the crystal lattice. Several theoretical models such as the double-exchange (DE) mechanism [5], small polarons, electron-lattice coupling, and especially, the Jahn–Teller (JT) type interaction [6–8], were proposed to explain the physics of CMR properties.

* Corresponding author.
E-mail addresses: wjlu@issp.ac.cn (W.J. Lu), ypsun@issp.ac.cn (Y.P. Sun).

0375-9601/$ – see front matter
doi:10.1016/j.physleta.2005.07.084

In contrast to the hole-doped materials, there have been a few electron-doped materials studied in this system. Zeng et al. [9] reported large negative magnetoresistance in electron-doped $Ca_{1-x}Ce_xMnO_3$ system. Low Ce doping stabilizes a ferromagnetic (FM) component in addition to a persistent antiferromagnetic (AFM) component. Higher Ce doping ($x \geqslant 0.075$) induces a charge ordering (CO) transition. The physical properties of $Ca_{1-x}Ce_xMnO_3$ are similar to those of hole-doped manganites [9,10]. However, Sundaresan et al. [11] have reported that the electron-doped $Sr_{1-x}Ce_xMnO_3$ does not show large negative magnetoresistance. Also the magnetic susceptibility (χ) versus T curve for $x > 0.10$ samples shows a broad maximum, which is absent in hole-doped manganites. They have explained this unusual behavior of χ using the dilute AFM model. Recently, Mandal et al. [12] prepared Ce doped $Sr_{1-x}Ce_xMnO_3$ by using a two step method and reported that the system did not show any long-range magnetic ordering but spin-glass like behavior at low temperatures for $x \geqslant 0.10$. For $x = 0.25$ and 0.35 samples, it shows large negative magnetoresistance over a wide range of T. The differences of the results in the last two papers should be due to the use of different ways for the sample preparation.

Anyway, the different electronic, and magnetic properties between electron-doped $Sr_{1-x}Ce_xMnO_3$ and hole-doped manganites have not fully been elucidated so far. Therefore, a detailed study of the crystallographic and magnetic phase diagram is needed. On the other hand, a potential intrinsic magnetic inhomogeneities in $Sr_{1-x}Ce_xMnO_3$ system should arouse our attention, since the evidence of inhomogeneities in manganites is very strong both in theory and experiments [13,14]. In this Letter, we studied the microscopically and intrinsically inhomogeneous magnetic phase in $Sr_{0.8}Ce_{0.2}MnO_3$ sample, for which a very broad maximum in $\chi(T)$ curve appears implying the dilute antiferromagnetism [11]. Here we use internal friction measurement technique to study the microscopic mechanism of magnetic phase transitions. The measurements, as discussed below, enable to obtain important information about magnetic phase separation.

The internal friction measuring technique is a non-destructive but very sensitive tool in studying defects and microscopic processes in solids including electron strongly correlated materials, such as cuprate high temperature superconductors and manganites [15–20]. By means of internal friction measurements, one may determine whether the microscopic process is phase transition or relaxation, and some other quantitative information such as activation energy and the relaxation time at infinite temperature can be obtained. In addition, the concomitant Young's modulus reflects the information of the lattice variation. The strong coupling of electron–phonon can be studied by the Young's modulus measurements. For $Sr_{0.8}Ce_{0.2}MnO_3$ sample, a remarkable peak in the internal friction curve is observed in the paramagnetic (PM) region, which is attributed to the formation of magnetic clusters. Furthermore, this peak is characteristic of thermally activated relaxation. The anomalous Young's modulus properties imply the electron–phonon interaction due to the JT effect may play an important role in the sample.

2. Experimental details

Polycrystalline $Sr_{0.8}Ce_{0.2}MnO_3$ sample was synthesized by the standard solid-state reaction. Stoichiometric precursor powders $SrCO_3$, CeO_2, MnO_2 and Cr_2O_3 were mixed and ground, then fired for 24 h at 1050 °C. The resultant powder was then pressed into small pellets and sintered at 1200 °C for 24 h and then at 1350 °C for another 24 h. After the final grinding, the powder was pressed into bars with the dimension of $65.0 \times 4.5 \times 1.0$ mm^3 (for internal friction and Young's modulus measurements), sintered at 1400 °C for 24 h and slow-cooled to room temperature.

The room temperature X-ray diffraction (XRD) measurement was taken in Philips X'pert PRO X-ray diffractometer with Cu K_α radiation. The structural parameters were obtained by fitting the experimental data of XRD using the standard Rietveld technique. The magnetic measurements were carried out with a Quantum Design superconducting quantum interference device (SQUID) MPMS system. The resistivity ρ was measured by means of a Quantum Design physical properties measurements system (PPMS) using the standard four-probe method. Internal friction $Q^{-1}(T)$ and Young's modulus $E(T)$ were measured by the free decay method of a resonant bar in acoustic frequency range with magnitude of kHz using warming mode in a vacuum environment at the rate of 1 K/min. The in-

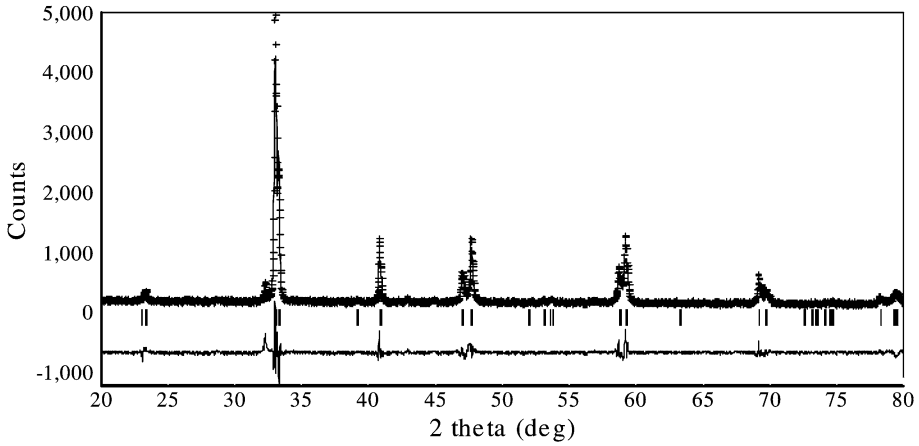

Fig. 1. XRD pattern of the compound $Sr_{0.8}Ce_{0.2}MnO_3$. Crosses indicate the experimental data and the calculated data is the continuous line overlapping them. The lowest curve shows the difference between experimental and calculated patterns. The vertical bars indicate the expected reflection positions.

ternal friction Q^{-1} is defined as follows [15]:

$$Q^{-1} = \frac{1}{n}\ln\left(\frac{A_0}{A_n}\right), \tag{1}$$

where n is the number of the vibration cycles, while the amplitude attenuates from A_0 to A_n. The Young's modulus E is given by

$$E = \frac{4\pi^2 sdl^4}{m^4 I} f^2, \tag{2}$$

where f is the resonant frequency, s the cross-sectional area, d the density, l the length, I the moment of inertia of the sample. In addition, m is 4.730 for the vibrating mode in the fundamental mode. According to the Eq. (2), E is proportional to the square of the resonant frequency f, i.e., $E \propto f^2$. Therefore, we substitute f^2 for the Young's modulus E.

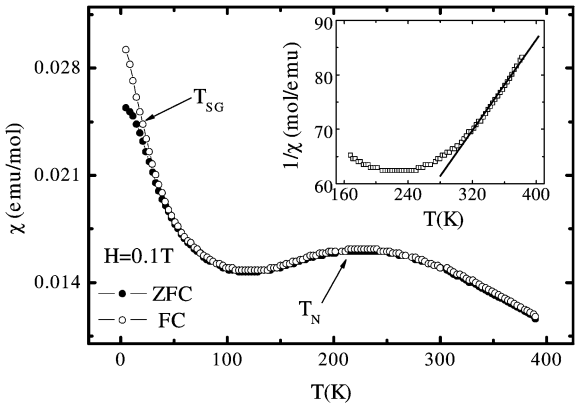

Fig. 2. Magnetic susceptibility, χ, as a function of temperature for $Sr_{0.8}Ce_{0.2}MnO_3$ under zero field cooling (ZFC) and field cooling (FC) at $H = 0.1$ T. Inset shows the inverse susceptibility. Solid line is the fitting data according to the Curie–Weiss law, $\chi = C/(T - \theta_P)$.

3. Results and discussion

XRD pattern of $Sr_{0.8}Ce_{0.2}MnO_3$ sample is shown in Fig. 1. The Rietveld refinements of the room temperature XRD pattern show that the sample is single phase with tetragonal structure (I4/mcm space group). The refined lattice parameters $a \approx b \approx 5.4013$ Å and $c \approx 7.7448$ Å, which are close to the reported values [11]. We have calculated Mn–O bond lengths and angles from the position of the ions in the unit cell and lattice parameters. The results show that there are two different bond lengths and angles. The difference between Mn–O1 and Mn–O2 bond lengths indicates that there is a strong Q_3-mode JT distortion of the MnO_6 octahedron and the doping electrons occupy the $d_{3z^2-r^2}$ orbital ordering.

The temperature dependence of magnetic susceptibility, $\chi(T)$, under an applied field of 0.1 T is shown in Fig. 2. ZFC and FC curves show that the sample is absent of long-range FM ordering. It undergoes a AFM transition at T_N (= 210 K), accompanied by a broad maximum, which indicates the dilute antiferromag-

netism. A short range FM interactions between Mn^{3+} and Mn^{4+} cannot be excluded, although there is no indication for a bulk ferromagnetism. In the absence of a FM ordering, the irreversibility between FC and ZFC at 20 K indicates a spin-glass (SG) like transition resulting from the AFM ordering and a short range FM interactions. In order to study the magnetic interaction further, we fit the experimental data in PM region according to the Curie–Weiss law, $\chi = C/(T - \theta_P)$. The temperature dependence of the inverse susceptibility, $1/\chi$, and the fitting curve are shown in the inset of Fig. 2. It is found that the Curie–Weiss law is not satisfactory with the experimental curve in the full PM temperature range. The deviation of the inverse susceptibility, $1/\chi$, from the high-temperature straight line corresponding to non-interacting magnetic moments (Curie–Weiss behaviour) marks the onset of the magnetic interaction between magnetic moments [21]. De Teresa et al. [22] observed the deviation of the inverse susceptibility from the Curie–Weiss law below $1.8T_C$ in PM region for $La_{0.67}Ca_{0.33}MnO_3$ compound, which signals the onset of short range FM correlation. They detected the presence of magnetic polarons (small magnetic clusters whose size is about 12 Å) in the PM state below $1.8T_C$ using small neutron scattering technique. For $Sr_{0.8}Ce_{0.2}MnO_3$ sample, the effective magnetic moment μ_{eff} deduced from experiment is about $5.96\mu_B$, which is larger than the calculated value ($4.10\mu_B$). Such a large μ_{eff} may be ascribed to the appearance of magnetic clusters in PM region. On the other hand, the positive Weiss constant θ_P ($\theta_P = 15$ K) approves the presence of short range FM interactions in PM region.

Fig. 3 shows $\ln\rho(T)$ curve for $Sr_{0.8}Ce_{0.2}MnO_3$ sample. The sample exhibits an insulating behavior in measuring temperature range. The temperature dependence of resistivity data is fitted by various models such as the adiabatic polaron hopping model $\rho \backsim T\exp(E/k_BT)$, the activated hopping model $\rho \backsim \exp(E/k_BT)$, and the variable range hopping (VRH) model $\rho \backsim \exp(T_0/T)^{1/4}$. It is found that the resistivity could be best fitted with the Mott's VRH model in large temperature range. The fitting result with VRH model is shown in the inset of Fig. 3. Fitting parameter T_0 obtained from the fitting result is 1.1×10^8 K. According Mott's VRH theory the parameter T_0 is inversely proportional to the localization length of the carriers. So the large value of T_0 implies a greater disorder exists in the sample. A fact is that in high temperature range ($T > 250$ K) polaron hopping model $\rho \backsim T\exp(E/k_BT)$ can better fit the data than VRH model. It has been reported that in PM region the resistivity of $La_{0.7}Ca_{0.3}MnO_3$ cannot be fitted with one conducting mechanism due to inhomogeneous magnetism [23]. For $Sr_{0.8}Ce_{0.2}MnO_3$, the different conducting mechanism in PM region may be due to the formation of FM clusters because of the JT distortion and the random potential fluctuations due to A-site cations.

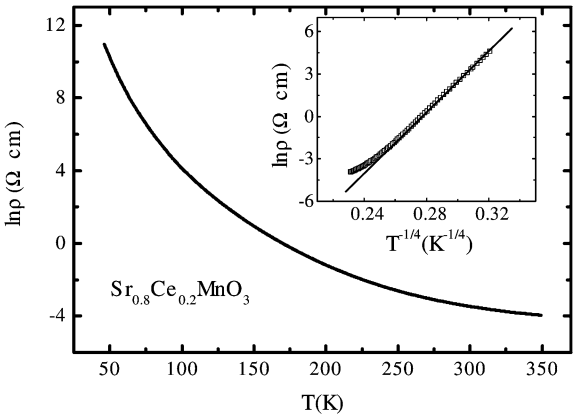

Fig. 3. T dependence of $\ln\rho$ for $Sr_{0.8}Ce_{0.2}MnO_3$. Inset shows the fitting plot of $\rho(T)$ curve according to the VRH model. The solid line represents the fitting data.

The results of internal friction and Young's modulus measurements under zero field are shown in Fig. 4(a) and (b). We define the resonant frequency at 300 K f_0. In the fundamental mode ($f_0 = 1516$ Hz), the internal friction (Q^{-1}) peak at 250 K is observed. In order to study the character of the Q^{-1} peak, $Q^{-1}(T)$ are measured in the first free flexural mode (changing the measuring frequency f to $2.76f$). The Q^{-1} peak shifts to higher temperature (262 K) with increasing measuring frequency, which demonstrates that the peak is associated with a thermally activated relaxation process. Combining with the results of susceptibility and resistivity, as discussed before, the peak should ascribe to the formation of FM clusters. In fact, the PM region appears to be dominated by local ferromagnetic fluctuations (FMF) that are presumably mediated by Mn^{3+}/Mn^{4+} hopping-induced DE interactions. The fluctuation in size or motion of the FM domain is generally accompanied by lattice dis-

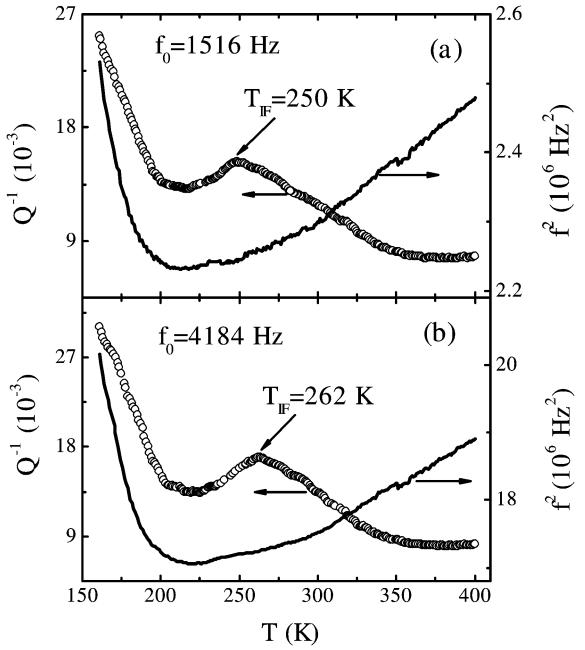

Fig. 4. Temperature dependence of internal friction Q^{-1} (empty circle) and Young's modulus $\Delta E \propto f^2$ (solid line) measured in (a) the fundamental mode ($f_0 = 1516$ Hz) (b) the first free flexural mode ($f_0 = 4184$ Hz). f_0 is defined the resonant frequency at 300 K. T_{IF} is the internal friction peak temperature.

tortion. If the deformation is inhomogeneous, the components with different lattice deformations have different mechanical properties, which result in stress concentration, the propagation of lattice deformation and motion of boundaries among different components. Thus, from a viewpoint of mechanics, the Q^{-1} peak in PM region can be induced. The similar Q^{-1} peak in $La_{1-x}Ca_xMnO_3$ were observed in PM region by other authors [18,24]. Ma et al. [24] observed Q^{-1} peak in $La_{2/3}Ca_{1/3}MnO_3$ in PM region, suggested to originate from the formation of the magnetic clusters.

In a thermally activated relaxation process, the internal friction of relaxation process can be described by Debye equation:

$$Q^{-1} = \Delta \frac{\omega\tau}{1+\omega^2\tau^2}, \tag{3}$$

where $\Delta = \delta E/E_0$, δE is the relaxation of the modulus, ω ($\omega = 2\pi f$) is the angular frequency, τ the relaxational time. In a typical thermally activated relaxation, the relation between τ and T can be expressed as $\tau = \tau_0 \exp(E_\alpha/k_B T)$, where E_α is the activation

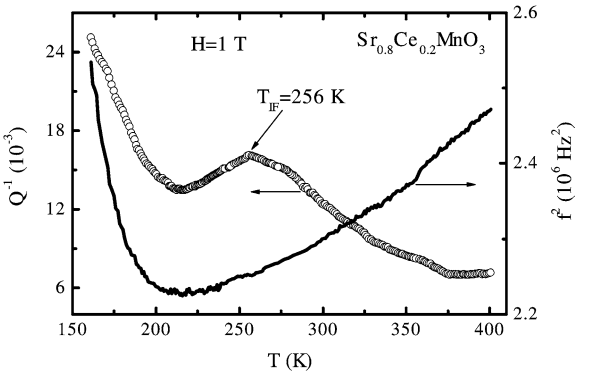

Fig. 5. Temperature dependence of internal friction Q^{-1} (empty circle) and Young's modulus $\Delta E \propto f^2$ (solid line) measured under applied magnetic field of $H = 1$ T. T_{IF} is the internal friction peak temperature.

energy, τ_0 is a constant, k_B is the Boltzman constant. The Q^{-1} is maximum when the $\omega\tau = 1$. Through the variation of the Q^{-1} peak temperature with respect to two different measured frequencies, the activation energy E_α can be calculated with the equation:

$$E_\alpha = k_B(\ln f_1 - \ln f_2)\left(\frac{1}{T_2} - \frac{1}{T_1}\right)^{-1}. \tag{4}$$

For $Sr_{0.8}Ce_{0.2}MnO_3$, the results are $E_\alpha \approx 0.45$ eV, $\tau_0 \approx 8.3 \times 10^{-14}$ s. Markovich et al. [25] observed phase separation phenomenon in $La_{0.82}Ca_{0.18}MnO_3$ single crystal below and above T_C, and calculated the volume of the FM cluster with the equation $\Delta E = KV$, where K is the magnetic anisotropy, V is the volume of the cluster, ΔE is activation energy deduced from ac susceptibility measured at different frequencies. Approximately, using the value of K ($\approx 10^5$ erg/cm^3) in Ref. [25], we can calculate that the size scale of the FM clusters in $Sr_{0.8}Ce_{0.2}MnO_3$ is about 20 nm. That is to say that the magnetic inhomogeneities result in nano-scale phase separation, which is similar to that observed in other manganites and cuprates materials [13,26].

In order to manifest that the internal friction peak is related to the formation of FM clusters, the $Q^{-1}(T)$ are measured under an applied magnetic field of 1 T. The results are shown in Fig. 5. The Q^{-1} peak move to higher temperature (256 K), which is consistent with the fact that the formation of FM clusters moves to higher temperature with such an applied magnetic field. Under applied magnetic field the movement of

the Q^{-1} peak testifies that peak is correlated with the intrinsic magnetic inhomogeneity, which is assuredly described as FM clusters in PM region.

Finally, we discuss the Young's modulus properties for this sample. In the vicinity of T_N, the Young's modulus E ($\propto f^2$) comes into being a valley and reaches a minimum value. In other words, there is a large softening of E in the vicinity of T_N. The Young's modulus E, microscopically, reflects the strain among the atoms. The elastic constant softening is the soft mode and reflects the instability of the lattice to a strain of a given symmetry [27,28]. The 3d electron state of transition-metal ions has an electric quadrupole moment due to the orbital state as well as a magnetic dipole moment. This softening should originate from the coupling of the orbital (quadrupolar) moment of the e_g orbital, $d_{3z^2-r^2}$ and $d_{x^2-y^2}$, of Mn^{3+} ion to the elastic strain [17,20]. The anomalous Young's modulus properties imply the electron–phonon coupling due to the JT effect may play an important role in the sample.

4. Conclusions

We have systematically studied the resistivity, magnetic, internal friction, and Young's modulus properties in $Sr_{0.8}Ce_{0.2}MnO_3$ sample. The experimental results prove the formation of the FM clusters in PM region, implying the intrinsic magnetic inhomogeneity. Nano-scale phase separation likely appears in the sample. The softening of Young's modulus indicates that there is a strong coupling of electron–phonon due to JT effect.

Acknowledgements

This work was supported by the National Key Research under Contract No. 001CB610604, and the National Nature Science Foundation of China under Contract Nos. 10374033 and 10474100, and the Fundamental Bureau, Chinese Academy of Sciences.

References

[1] S. Jin, T.H. Tiefel, M. McCormack, R.A. Fastnacht, R. Ramesh, L.H. Chen, Science 264 (1994) 413.
[2] Y. Tokura, Y. Tomioka, H. Kuwahara, A. Asamitsu, Y. Moritomo, M. Kasai, J. Appl. Phys. 79 (1996) 5288.
[3] Y. Tokura, Colossal Magnetoresistance Oxides, Gordon and Breach, New York, 2000.
[4] J.M.D. Coey, M. Viret, S. Von Molnár, Adv. Phys. 48 (1999) 167.
[5] C. Zener, Phys. Rev. 82 (1951) 403;
P.W. Anderson, H. Hasegawa, Phys. Rev. 100 (1955) 675.
[6] A.J. Millis, P.B. Littlewood, B.I. Shraiman, Phys. Rev. Lett. 74 (1995) 5144.
[7] H. Röder, J. Zang, A.R. Bishop, Phys. Rev. Lett. 76 (1996) 1356.
[8] A.J. Millis, B.I. Shraiman, R. Mueller, Phys. Rev. Lett. 77 (1996) 175.
[9] Z. Zeng, M. Greenblatt, M. Croft, Phys. Rev. B 63 (2001) 224410.
[10] A. Maigan, C. Martin, F. Damay, B. Raveau, Chem. Mater. 10 (1998) 950.
[11] A. Sundaresan, J.L. Tholence, A. Maignan, C. Martin, M. Hervieu, B. Raveau, E. Suard, Eur. Phys. J. B 14 (2000) 431.
[12] P. Mandal, A. Hassen, A. Loidl, Phys. Rev. B 69 (2004) 224418.
[13] E. Dagotto, J. Burgy, A. Moreo, Solid State Commun. 126 (2003) 9.
[14] A. Moreo, S. Yunoki, E. Dagotto, Science 283 (1999) 2034.
[15] J. Du, Y. Sun, J. Jiang, F. Zeng, H. Yin, Phys. Rev. B 41 (1990) 6679.
[16] R.I. Zainullina, N.G. Bebinin, A.M. Burkhanov, V.V. Ustinov, Y.M. Mukovskii, Phys. Rev. B 66 (2002) 64421.
[17] R.K. Zheng, R.X. Huang, A.N. Tang, G. Li, X.G. Li, J.N. Wei, J.P. Shui, Z. Yao, Appl. Phys. Lett. 81 (2002) 3834.
[18] J. Mira, J. Rivas, A. Moreno-Gobbi, M. Pérez Macho, G. Paolini, F. Rivadulla, Phys. Rev. B 68 (2003) 92404.
[19] F. Cordero, C. Castellano, R. Cantelli, M. Ferretti, Phys. Rev. B 65 (2001) 12403.
[20] Y.Q. Ma, W.H. Song, R.L. Zhang, J.M. Dai, J. Yang, J.J. Du, Y.P. Sun, C.Z. Bi, Y.J. Ge, X.G. Qiu, Phys. Rev. B 69 (2004) 134404.
[21] M.T. Causa, et al., Phys. Rev. B 58 (1998) 3233.
[22] J.M. De Teresa, M.R. Ibarra, P.A. Algarabel, C. Ritter, C. Marquina, J. Blasco, J. Garcia, A. del Moral, Z. Arnold, Nature 386 (1997) 256.
[23] P.S. Anil Kumar, P.A. Joy, S.K. Date, J. Phys.: Condens. Matter 10 (1998) L269.
[24] Y.Q. Ma, W.H. Song, J. Yang, B.C. Zhao, R.L. Zhang, Z.G. Sheng, W.J. Lu, G.H. Zheng, J.M. Dai, J.J. Du, Y.P. Sun, J. Phys.: Condens. Matter 16 (2004) 7083.
[25] V. Markovich, et al., Phys. Rev. B 65 (2002) 144402.
[26] E. Dagotto, T. Hotta, A. Moreo, Phys. Rep. 344 (2001) 1.
[27] M. Kataoka, J. Phys. Soc. Jpn. 70 (2001) 2353.
[28] M. Saint-Paul, P. Lejay, Physica B 352 (2004) 353.